J Mater Sci: Mater Electron (2017) 28:1301–1306
DOI 10.1007/s10854-016-5659-y

Hydrothermal synthesis of $NaLa(WO_4)_2:Eu^{3+}$ octahedrons and tunable luminescence by changing Eu^{3+} concentration and excitation wavelength

Yanxia Tang[1] · Yongfei Ye[2] · Haihui Liu[3] · Xiongfei Guo[3] · Hongxia Tang[4] · Wenzhong Yin[1] · Yaping Gao[1]

Received: 6 July 2016 / Accepted: 29 August 2016 / Published online: 1 September 2016

Abstract $NaLa(WO_4)_2:Eu^{3+}$ phosphors with different Eu^{3+} concentrations have been synthesized by a hydrothermal method. The phase is confirmed by XRD analysis, which shows a pure-phase $NaLa(WO_4)_2$ XRD pattern for all of $NaLa(WO_4)_2:Eu^{3+}$ phosphors. The SEM and TEM images indicate that all of $NaLa(WO_4)_2:Eu^{3+}$ phosphors have a octahedral morphology. These suggest that the Eu^{3+} doping has no influence on the structure and growth of $NaLa(WO_4)_4$ particles. By monitoring the emission of Eu^{3+} at 615 nm, $NaLa(WO_4)_2:Eu^{3+}$ phosphors show excitation bands originating from both host and Eu^{3+} ions. Under the excitation at 271 nm corresponding to WO_4^{2-} groups, emission bands coming from the $^1A_1 \rightarrow {}^3T_1$ transition with the WO_4^{2-} groups and the $^5D_0 \rightarrow {}^7F_j$ (j = 0, 1, 2, 3 and 4) transitions of Eu^{3+} are observed. The emission intensity relating to WO_4^{2-} groups decreases with increasing Eu^{3+} concentration. But emission intensities of Eu^{3+} increase firstly and then decreases because of concentration quenching effect. Under the excitation at 395 nm corresponding to $^7F_0 \rightarrow {}^5L_6$ transition of Eu^{3+}, only characteristic Eu^{3+} emission bands can be observed. The results of this work suggest that tunable luminescence can be obtained for Eu^{3+} doped $NaLa(WO_4)_2$ phosphors by changing Eu^{3+} concentration and excitation wavelength.

✉ Hongxia Tang
hxtanghb@sina.com

[1] College of Science, Hebei North University, Zhangjiakou 075000, China

[2] College of Information Science and Engineering, Hebei North University, Zhangjiakou 075000, China

[3] The Nineteenth Middle School of Zhangjiakou, Hebei 075000, China

[4] Department of Endocrinology, Zhangjiakou First Hospital, Zhangjiakou 075000, China

1 Introduction

More and more attentions are paid to phosphor materials in recent years due to their applications in fields of solid state lighting [1], solar cells [2], sensors [3], medical and biological labels [4]. To meet the requirements of these applications, phosphors materials are expected to show high-efficiency and color controllable emissions, high physical and chemical stabilities, and so on. The luminescent properties of phosphor materials are affected by some factors, such as host, excitation wavelength, temperature, size and morphology. Rare earth ions play an important role in phosphor materials owing to their abundant emission colors originating from the 4*f*–4*f* or 5*d*–4*f* transitions [5]. For example, as one of widely used activators of red emission, Eu^{3+} often shows emission bands originating from $^5D_0 \rightarrow {}^7F_j$ (j = 0, 1, 2, 3 and 4) transitions, whereas the relative intensity of these emission bands are influenced highly by the site of Eu^{3+} in the host. There will be a relative strong $^5D_0 \rightarrow {}^7F_1$ transition and a relative weak $^5D_0 \rightarrow {}^7F_2$ transition when Eu^{3+} locates a site without an inversion [6].

Double tungstates with the formula of $MRE(WO_4)_2$ (M = alkali-metal ions, RE = rare earth ions) are considered as potent candidates for the excellent physical and chemical stability and luminous efficiency [7]. The efficient energy transfer from the host matrix to the localized states of lanthanide ions also benefits the luminescent property. These materials have the scheelitr-type structure and contain the WO_4^{2-} tetrahedral anions (W^{6+} is coordinated by four oxygen atoms in a tetrahedral site, and the

RE^{3+}/M^{+} site is eight coordinated). They exhibit excellent luminescence-property and can meet the various demands for exploring high-quality phosphor materials when they are doped with rare earth ions. A large number of rare earth ions doped double tungstates, such as $NaGd(WO_4)_2$:Tb^{3+} [8], $NaLu(WO_4)_2$:Eu^{3+} [2], $NaLa(WO_4)_2$:Er^{3+}/Yb^{3+} [9], $NaLa(WO_4)_2$:$Eu^{3+}/Tb^{3+}/Tm^{3+}$ [10], $NaGd(WO_4)_2$:Ho^{3+}/Yb^{3+} [11] and $NaGd(WO_4)_2$:$Tm^{3+}/Dy^{3+}/Eu^{3+}$ [12], have been synthesized successfully by different methods.

In this wok, we report on the hydrothermal synthesis of $NaLa(WO_4)_2$:Eu^{3+} phosphors. Hydrothermal method, as a typical solution-based approach, has been proved to be an effective and convenient synthesis technique for preparing uniform and well-dispersed phosphor particles. The hydrothermal process can be controlled by an appropriate choice of reaction parameters, such as temperature, time, pH value and surfactant. Moreover, low reaction temperature, mild reaction conditions, size-selective growth, controllable morphology, phase purity, smaller particle size, and narrow particle size distribution are the advantages of the hydrothermal synthesis method. We find that the obtained $NaLa(WO_4)_2$:Eu^{3+} phosphors have the octahedral morphology and the luminescence can be tuned by changing Eu^{3+} concentration and excitation wavelength.

2 Materials and methods

A series of $NaLa(WO_4)_2$:x mol%Eu^{3+} (x = 0, 3, 6, 9, 12 and 15) phosphors were synthesized by a hydrothermal process. La_2O_3 (99.99 %), Eu_2O_3 (99.99 %), $(NH_4)_6W_7O_{24}{\cdot}6H_2O$ (AR) and $NaNO_3$ (AR) were used as raw materials. NaOH (AR) was used to adjust the pH values. All raw materials were used directly without further purification. $La(NO_3)_3$ and $Eu(NO_3)_3$ solutions were obtained firstly by dissolving La_2O_3 and Eu_2O_3 into HNO_3 with constant stirring and heating at about 50 °C until all materials were dissolved completely. The mole ratios of Eu_2O_3:La_2O_3 were 0, 3:97, 6:94, 9:91, 12:88 and 15:85, respectively. Then, $(NH_4)_6W_7O_{24}{\cdot}6H_2O$ and $NaNO_3$ were added to the above solution with stirring for about 30 min. The pH value of solution was adjusted to be 7 by adding appropriate NaOH, which induces the formation of suspension solution. The suspension solution was subsequently transferred into a 100 ml Teflon vessel and sealed in a stainless steel autoclave. The autoclave with its contents was treated under hydrothermal conditions for 10 h at 180 °C. When the reaction was completed, it was naturally cooled to room temperature and a white precipitate was obtained. Afterwards, the precipitates were filtered by centrifugation and washed several times using deionized water and ethanol. The final products were dried at 70 °C for 24 h in air.

The X-ray powder diffraction (XRD) measurements were carried out on a Rigaku-Dmax 2500 diffractometer using Cu Kα radiation (λ = 0.15405 nm). The morphologies and microstructures were studied by scanning electron microscopy (SEM, Hitachi S-4800) and transmission electron microscopy (TEM, JEOL-2100F). Selected-area electron diffraction (SAED) and high-resolution TEM (HRTEM) were examined on a JEM-2010F high-resolution transmission electron microscope. The luminescence was performed on a HitachiF-7000 spectrophotometer equipped with a 150 W xenon lamp as the excitation source.

3 Results and discussion

The phase of obtained $NaLa(WO_4)_2$:Eu^{3+} phosphors has been confirmed by XRD analysis. It is clear from Fig. 1 that all diffractions are well according with the pure-phase $NaLa(WO_4)_2$ (JCPDS No. 79-1118) and no secondary phase is detected. This indicates that the phosphors doped with different Eu^{3+} concentrations remain a single phase. According to the effective ionic radii of cations, Eu^{3+} (1.066 Å for CN = 8) ions are proposed to occupy the sites of La^{3+} (1.160 Å for CN = 8) or Na^{+} (1.180 Å for CN = 8). However, on the basis of the valence state analysis, the Eu^{3+} ions are much more probably occupying the La^{3+} sites. The diffraction peaks shift slightly to higher 2θ angles with the increasing Eu^{3+} concentrations because of the substitution of La^{3+} by Eu^{3+} and the smaller ionic radius of Eu^{3+} comparing with La^{3+}. The lattice parameters were calculated using least square refinement program CHECKCELL. The calculated lattice parameter as a function of Ca concentration is shown in Fig. 2. The above results suggest that the Eu^{3+} ions have been effectively incorporated into the host lattices by replacing La^{3+} sites without altering the host structure and the well-crystallized

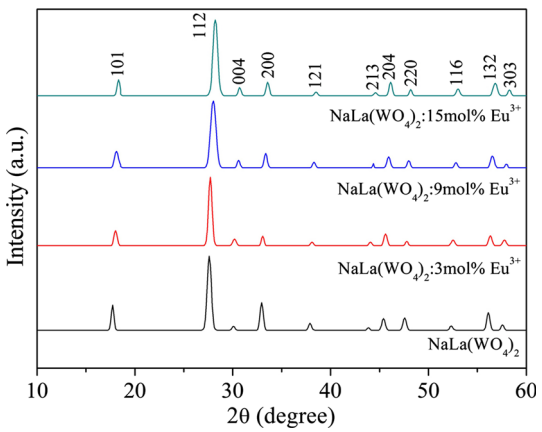

Fig. 1 XRD patterns of pure $NaLa(WO_4)_2$ and Eu^{3+} doped $NaLa(WO_4)_2$ phosphors

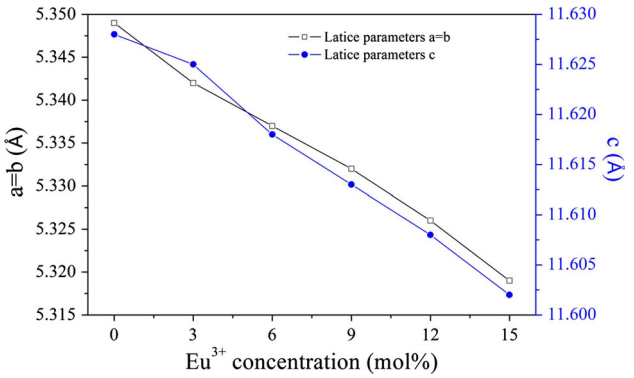

Fig. 2 Lattice parameters of $NaLa(WO_4)_2$:x mol%Eu^{3+} (x = 0, 3, 6, 9, 12 and 15) phosphors

$NaLa(WO_4)_2$:Eu^{3+} samples can be obtained under the present hydrothermal conditions.

Figure 3 gives the SEM (Fig. 3a) and TEM (Fig. 3b) images of $NaLa(WO_4)_2$:12 mol%Eu^{3+} phosphors. From images, one can see that monodispersed particles with a well-defined octahedral morphology are obtained. Generally, the Ostwald ripening process is a well accepted mechanism for the crystal growth. In the Ostwald ripening process, the initial formation of tiny crystalline nuclei in a supersaturated medium is followed by crystal growth. In this process the larger particles grow at the cost of the small ones due to the energy difference between large particles and small particles. Initially, the mixture solution containing $La(NO_3)_3$, $Eu(NO_3)_3$, $NaNO_3$ and $(NH_4)_6W_7O_{24}$ with a pH value of 7 yields the formation of abundant amorphous $NaLa(WO_4)_2$:Eu^{3+} particles, which serves as precursors of the crystal. Next, the hydrothermal process induces the crystallization, in which amorphous particles nucleate and hydroxyl anions are adsorbed selectively. Finally, the crystal grows with certain faces and octahedral crystals are formed. All of $NaLa(WO_4)_2$:Eu^{3+} phosphors with different Eu^{3+} concentrations have similar morphology, indicating that the Eu^{3+} concentration has no influence on morphology. The bright spots in the SAED pattern (Fig. 3c) demonstrate the single crystalline nature of $NaLa(WO_4)_2$:12 mol%Eu^{3+} phosphors, which is in accordance with the clear lattice fringes in the HRTEM image in Fig. 3d. Additionally, the distance between two adjacent lattice fringes was calculated to be 0.294 nm, which corresponds with the (004) plane of tetragonal $NaLa(WO_4)_2$.

Figure 4 shows the excitation spectra of $NaLa(WO_4)_2$ and $NaLa(WO_4)_2$:12 mol%Eu^{3+} phosphors by monitoring 615 nm emission of Eu^{3+}. Both $NaLa(WO_4)_2$ and $NaLa(WO_4)_2$:12 mol%Eu^{3+} phosphors have a strong and broad band ranging from 200 to 350 nm with a maximum at about 271 nm, which is the charge transfer band (CTB)

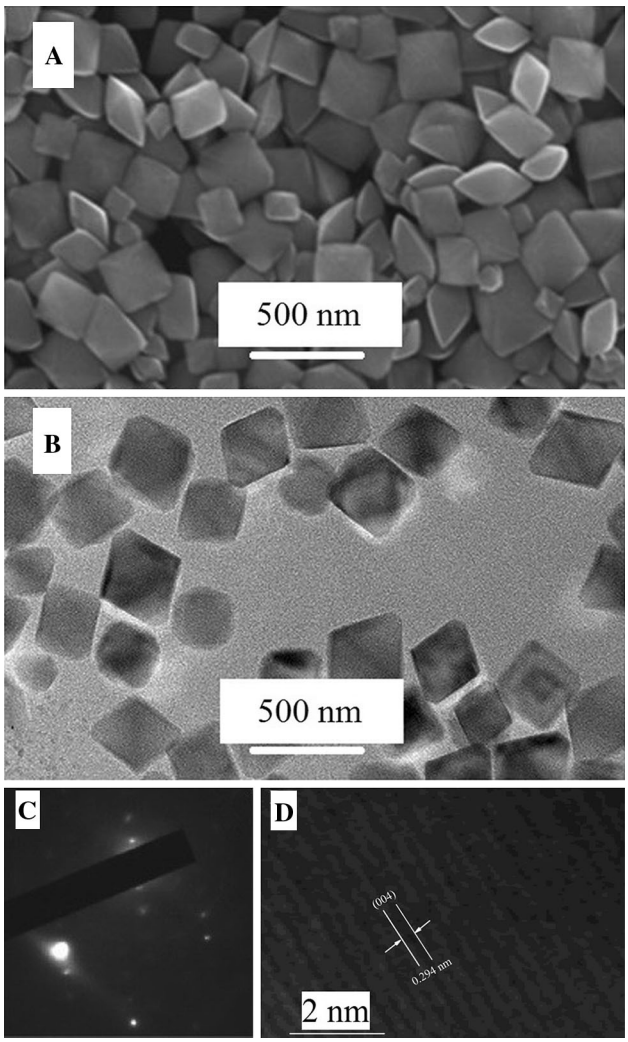

Fig. 3 SEM (**a**), TEM (**b**), SAED pattern (**c**) and HRTEM (**d**) images of $NaLa(WO_4)_2$:12 mol%Eu^{3+} phosphor

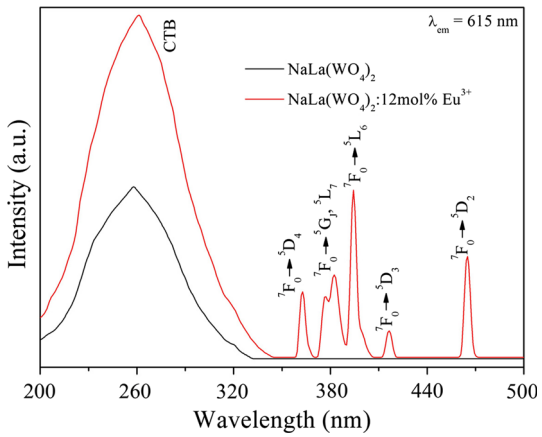

Fig. 4 Excitation spectra of $NaLa(WO_4)_2$ and $NaLa(WO_4)_2$:12 mol%Eu^{3+} phosphor

of WO_4^{2-} groups and $O^{2-} \rightarrow Eu^{3+}$ transition from an oxygen 2*p* state excited to an Eu^{3+} 4*f* state. Mostly, the contribution of these two transitions cannot be distinguished obviously because of the spectral overlap. For $NaLa(WO_4)_2$:12 mol%Eu^{3+}, a series of sharp excitation lines in the range of 350–500 nm also can be observed, which is the typical intra-4*f* transitions of Eu^{3+}. The excitation lines in this region come from $^7F_0 \rightarrow {}^5D_4$, $^7F_0 \rightarrow {}^5G_J$, $^7F_0 \rightarrow {}^5L_7$, $^7F_0 \rightarrow {}^5L_6$, $^7F_0 \rightarrow {}^5D_3$ and $^7F_0 \rightarrow {}^5D_2$ transitions of Eu^{3+}, respectively. Herein, the presence of excitation band of WO_4^{2-} groups by monitoring Eu^{3+} emission suggests an energy transfer from WO_4^{2-} groups to Eu^{3+}.

Figure 5 shows the emission spectra of $NaLa(WO_4)_2$: x mol%Eu^{3+} (x = 0, 3, 6, 9, 12 and 15) phosphors under an excitation at 271 nm. All of Eu^{3+} doped $NaLa(WO_4)_2$ phosphors have similar profiles and each one consists of two parts: one is the broad band in the range of 350–575 nm with a maximum at about 468 nm and the other consists of several emission lines in the range of 575–725 nm. The broad band peaking at about 468 nm is due to the $^1A_1 \rightarrow {}^3T_1$ transition with the WO_4^{2-} groups. The pure $NaLa(WO_4)_2$ only has this emission band under excitation at 271 nm. The sharp emission bands with maximum at 590, 599, 615, 623 and 706 nm result from the $^5D_0 \rightarrow {}^7F_j$ (j = 0, 1, 2, 3 and 4) transitions of Eu^{3+}, respectively. The emission band peaking at 615 nm (originating from the $^5D_0 \rightarrow {}^7F_2$ electric dipole transition of Eu^{3+}) is strongest, suggesting that Eu^{3+} locates a non-symmetry site in $NaLa(WO_4)_2$ host. For $NaLa(WO_4)_2$:Eu^{3+} phosphors, the emission intensity of the host decreases gradually with increasing Eu^{3+} concentrations. The emission intensity corresponding to Eu^{3+} increases with increasing Eu^{3+} concentrations and reaches a maximum at x = 12. The concentration of Eu^{3+} more than 12 mol% in $NaLa(WO_4)_2$ host induces the decrease of Eu^{3+} emission due to the concentration quenching effect. The changes of emission intensity relating to transition of host and Eu^{3+} confirm the existence of energy transfer from the host to Eu^{3+} in $NaLa(WO_4)_2$:Eu^{3+} phosphors. But WO_4^{2-} groups do not transfer all of the absorbed energy to Eu^{3+} ions so that the emission of host can be observed. Also, such energy transfer phenomenon demonstrates that the as-synthesized $NaLa(WO_4)_2$:Eu^{3+} is a solid solution, in which Eu^{3+} has successfully incorporated into $NaLa(WO_4)_2$ lattice, agreeing well with the XRD results [13].

Figure 6 shows the emission spectra of $NaLa(WO_4)_2$: x mol%Eu^{3+} (x = 0, 3, 6, 9, 12 and 15) phosphors under excitation at 395 nm. The results show that the excitation wavelength has obvious influence on the luminescence of $NaLa(WO_4)_2$:Eu^{3+} phosphors. There are only characteristic emission bands of Eu^{3+} ions, indicating that the energies absorbed by the $^7F_0 \rightarrow {}^5L_6$ transition cannot be transferred to WO_4^{2-} groups. This advises that excitation induced emissions are possible from the single emitting component by dissolving the suitable amount of Eu^{3+} ions in the calcium site due to WO_4 polarization in the luminescence. This result is similar to that of $CaMoO_4$:Eu^{3+} phosphors reported by Raju et al. [14]. But the dependence of Eu^{3+} emission on the Eu^{3+} concentration is similar to those of results obtained by 271 nm excitation.

In order to determine the energy transfer mechanism from host to activators in $NaLa(WO_4)_2$:Eu^{3+} phosphors, it is necessary to know the critical distance (R_c) between the neighbouring Eu^{3+} ions. The critical transfer distance (R_c) can be calculated by the formula of $R_C \approx 2(3V/4\pi XN)^{\frac{1}{3}}$, where X is the critical concentration of Eu^{3+}, V is the volume of the unit cell, and N is the number of available sites of the dopant in the unit cell [15]. For $NaLa(WO_4)_2$ host, the values of V, X and N are 332.698 $Å^3$, 0.12 and 2, respectively. The critical distance is calculated to be about

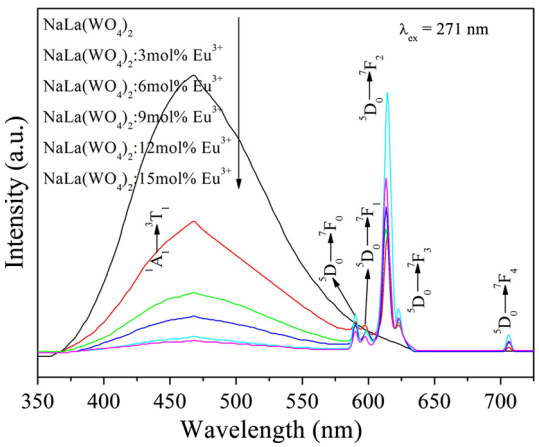

Fig. 5 Emission of $NaLa(WO_4)_2$:x mol%Eu^{3+} (x = 0, 3, 6, 9, 12 and 15) phosphors under excitation at 271 nm

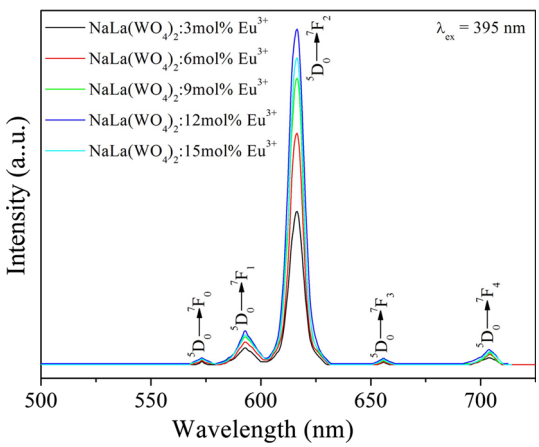

Fig. 6 Emission of $NaLa(WO_4)_2$:x mol%Eu^{3+} (x = 0, 3, 6, 9, 12 and 15) phosphors under excitation at 395 nm

13.86 Å. With the increase of Eu^{3+} concentration, the energy transfer from the host to Eu^{3+} becomes more efficient, and the probability of energy migration between activators increases simultaneously. When the distance becomes small enough, the concentration quenching phenomenon takes place and the energy migration is hindered. In general, there are two main mechanisms for a non-radiative energy transfer process: one is exchange interaction, and the other is electric multipolar interactions [16]. The value of R_c acquired above indicates the little possibility of exchange interaction since it can be predominant only for about 5 Å. Hence, we can conclude that the energy transfer mechanism from the host to Eu^{3+} is dominated by the electric multipolar interactions.

It is well known that the intensities of the transitions between different J-number levels are dependent on the symmetry of the local environment of Eu^{3+} activators in terms of the Judd–Ofelt theory [6, 17]. The magnetic dipole transition ($^5D_0 \rightarrow {}^7F_1$, orange emission) will dominate if Eu^{3+} is in a site with inversion symmetry, whereas electric dipole transition ($^5D_0 \rightarrow {}^7F_2$, red emission) dominates when Eu^{3+} locates a site without inversion symmetry. Therefore, the luminescent intensity ratio of $^5D_0 \rightarrow {}^7F_2$ to $^5D_0 \rightarrow {}^7F_1$ (R/O) is used to measure the degree of distortion from inversion symmetry of the local chemical environment surrounding Eu^{3+} in the host. As shown in Figs. 4 and 5, the emission intensity of $^5D_0 \rightarrow {}^7F_2$ is much higher than that of $^5D_0 \rightarrow {}^7F_1$ for $NaLa(WO_4)_2$:Eu^{3+} phosphors. The R/O values of $NaLa(WO_4)_2$:Eu^{3+} phosphors with different Eu^{3+} concentrations are shown in Fig. 7. It reveals that the R/O values increase with the increasing Eu^{3+} concentrations, indicating Eu^{3+} occupies more distorted local environment. The color purity of Eu^{3+} doping phosphors can be characterized as the R/O value [18].

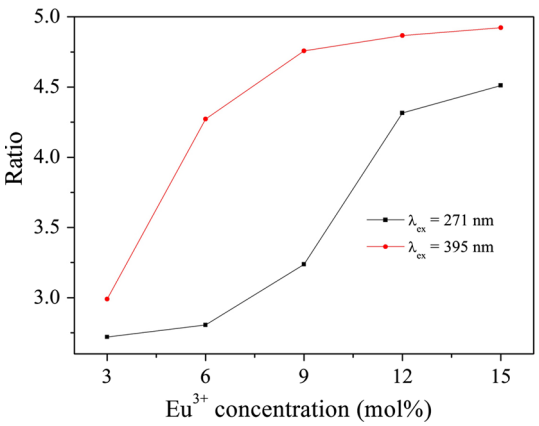

Fig. 7 Dependence of the luminescent intensity ratio of $^5D_0 \rightarrow {}^7F_2$ to $^5D_0 \rightarrow {}^7F_1$ on Eu^{3+} concentration

4 Conclusion

We have synthesized a series of $NaLa(WO_4)_2$:Eu^{3+} phosphors by a hydrothermal method. The Eu^{3+} doping has no influence on the phase structure and morphology of obtained $NaLa(WO_4)_2$:Eu^{3+} samples. The Eu^{3+} concentration in $NaLa(WO_4)_2$ host and the excitation wavelength have obvious influence on luminescence of $NaLa(WO_4)_2$:Eu^{3+} phosphors. Under the excitation at 271 nm corresponding to WO_4^{2-} groups, emission bands coming from the $^1A_1 \rightarrow {}^3T_1$ transition with the WO_4^{2-} groups and the $^5D_0 \rightarrow {}^7F_j$ (j = 0, 1, 2, 3 and 4) transitions of Eu^{3+} are observed. The emission intensity relating to WO_4^{2-} groups decreases with increasing Eu^{3+} concentration. But emission intensities of Eu^{3+} increase firstly and then decreases because of concentration quenching effect. Under the excitation at 395 nm corresponding to $^7F_0 \rightarrow {}^5L_6$ transition of Eu^{3+}, only characteristic Eu^{3+} emission bands can be observed. The results of this work suggest that tunable luminescence can be obtained for Eu^{3+} doped $NaLa(WO_4)_2$ phosphors by changing Eu^{3+} concentration and excitation wavelength.

Acknowledgments This work is financially supported by the General Project of Hebei North University (Nos. 2013003 and S201407), Science and Technology Department of Hebei Province Project (No. 16961301D), Zhangjiakou Science and Technology Bureau Projects (Nos. 13110038I-3, 12110058E−4, 11110024D and 1511075B), the Social Science Fund of Heibei Province (No. HB14JY075) and Health Department of Hebei Province Project (No. 20160030).

References

1. Y.Y. Cao, N.D. Liu, J. Tian, X. Zhang, Polyhedron **107**, 78 (2016)
2. Y.M. Wang, H.B. Zhang, S.S. Qu, C.H. Su, J. Alloys Compd. **677**, 266 (2016)
3. Z. Wei, W. Zheng, Z.Y. Zhu, X.F. Guo, Chem. Phys. Lett. **651**, 46 (2016)
4. Y.X. Tang, R. Mei, S.K. Yang, H.X. Tang, W.Z. Yin, Y.C. Xu, Y.P. Gao, Superlattices Microstruct. **92**, 256 (2016)
5. P. Li, U. Liu, Y.X. Guo, X.L. Shi, G.Q. Zhu, H.Q. Zuo, Ceram. Int. **41**, 6620 (2015)
6. Y.G. Yang, Mater. Sci. Eng. B **178**, 807 (2013)
7. Z.J. Wang, J.P. Zhong, H.X. Jiang, J. Wang, H.B. Liang, Cryst. Growth Des. **14**, 3767 (2014)
8. Y.X. Liu, X.J. Yue, K. Cai, H.D. Deng, M. Zhang, Energy **93**, 1413 (2015)
9. X.L. Liu, W.H. Hou, X.Y. Yang, Q.M. Shen, RSC Adv. **42**, 11445 (2013)
10. X.L. Liu, W.H. Hou, X.Y. Yang, J.Y. Liang, CrystEngComm **16**, 1268 (2014)
11. X.C. Yu, Y.B. Qin, M.L. Gao, L. Duan, Z.Q. Jiang, L. Gou, P. Zhao, Z. Li, J. Lumin. **153**, 1 (2014)
12. Y. Liu, G.X. Liu, J.X. Wang, X.T. Dong, W.S. Yu, Inorg. Chem. **53**, 11457 (2014)
13. Y. Zhang, W.T. Gong, J.G. Yu, Z.Y. Cheng, G.L. Ning, RSC Adv. **6**, 30886 (2016)

14. G.S.R. Raju, E. Pavitra, Y.H. Ko, J.S. Yu, J. Mater. Chem. **22**, 15562 (2012)
15. Z.-W. Zhang, A.-J. Song, S.-T. Song, J.-P. Zhang, W.-G. Zhang, D.-J. Wang, J Alloys Compd. **629**, 32 (2015)
16. L.G. Van Uitert, J. Electrochem. Soc. **114**, 1048 (1967)
17. A. Zaushitsyn, V. Mikhailin, A. Romanenko, E. Khaikina, O. Basovich, V. Morozov, B. Lazoryak, Inorg. Mater. **41**, 766 (2005)
18. R. Krishnan, J. Thirumalai, S. Thomas, M. Gowri, J. Alloys Compd. **604**, 20 (2014)